



Delft University of Technology

Tight MIP formulations of the power-based unit commitment problem

Morales-España, Germán; Gentile, Claudio; Ramos, Andres

DOI

[10.1007/s00291-015-0400-4](https://doi.org/10.1007/s00291-015-0400-4)

Publication date

2015

Document Version

Final published version

Published in

OR Spectrum

Citation (APA)

Morales-España, G., Gentile, C., & Ramos, A. (2015). Tight MIP formulations of the power-based unit commitment problem. *OR Spectrum*, 37(4), 929-950. <https://doi.org/10.1007/s00291-015-0400-4>

Important note

To cite this publication, please use the final published version (if applicable). Please check the document version above.

Copyright

Other than for strictly personal use, it is not permitted to download, forward or distribute the text or part of it, without the consent of the author(s) and/or copyright holder(s), unless the work is under an open content license such as Creative Commons.

Takedown policy

Please contact us and provide details if you believe this document breaches copyrights. We will remove access to the work immediately and investigate your claim.

Tight MIP formulations of the power-based unit commitment problem

Germán Morales-España¹  · Claudio Gentile² ·
Andres Ramos³

Received: 1 December 2014 / Accepted: 15 April 2015 / Published online: 23 May 2015
© The Author(s) 2015. This article is published with open access at Springerlink.com

Abstract This paper provides the convex hull description for the basic operation of slow- and quick-start units in power-based unit commitment (UC) problems. The basic operating constraints that are modeled for both types of units are (1) generation limits and (2) minimum up and down times. Apart from this, the startup and shutdown processes are also modeled, using (3) startup and shutdown power trajectories for slow-start units, and (4) startup and shutdown capabilities for quick-start units. In the conventional UC problem, power schedules are used to represent the staircase energy schedule; however, this simplification leads to infeasible energy delivery, as stated in the literature. To overcome this drawback, this paper provides a power-based UC formulation drawing a clear distinction between power and energy. The proposed

The work of G. Morales-España was supported by the Cátedra Iberdrola de Energía e Innovación (Spain). The work of C. Gentile was partially supported by (1) the project MINO Grant No. 316647 Initial Training Network of the “Marie Curie” program funded by the European Union and also (2) the PRIN project 2012 “Mixed-Integer Nonlinear Optimization: Approaches and Applications”.

✉ Germán Morales-España
g.a.moralesespana@tudelft.nl
Claudio Gentile
gentile@iasi.cnr.it
Andres Ramos
andres.ramos@upcomillas.es

¹ Department of Electrical Sustainable Energy, Delft University of Technology, 2628 CD Delft, The Netherlands

² Istituto di Analisi dei Sistemi ed Informatica “A. Ruberti”, C.N.R., Via dei Taurini 19, 00185 Roma, Italy

³ Institute for Research in Technology (IIT) of the School of Engineering (ICAI), Universidad Pontificia Comillas, Madrid, Spain

constraints can be used as the core of any power-based UC formulation, thus tightening the final mixed-integer programming UC problem. We provide evidence that dramatic improvements in computational time are obtained by solving different case studies, for self-UC and network-constrained UC problems.

Keywords Convex hull · Unit commitment (UC) · Mixed-integer programming (MIP) · Tight formulation · Slow-start units · Quick-start units

1 Introduction

The short-term unit commitment (UC) problem is one of the critical tasks that is daily performed by different actors in the electricity sector. Depending on the purpose, the UC is solved under centralized or competitive environments, from self-scheduling to centralized auction-based market clearing, over a time horizon ranging from one day to one week.

In general, the UC main objective is to meet demand at minimum cost while operating the system and units within secure technical limits [4, 11, 22]. The UC problem can then be defined as:

$$\begin{aligned} \min_{\mathbf{x}, \mathbf{p}} \quad & \mathbf{b}^\top \mathbf{x} + \mathbf{c}^\top \mathbf{p} \\ \text{s.t.} \quad & \mathbf{F}\mathbf{x} \leq \mathbf{f}, \mathbf{x} \text{ is binary} & (1) \\ & \mathbf{H}\mathbf{p} \leq \mathbf{h} & (2) \\ & \mathbf{A}\mathbf{x} + \mathbf{B}\mathbf{p} \leq \mathbf{g}, & (3) \end{aligned}$$

where \mathbf{x} and \mathbf{p} are decision variables. The binary variable \mathbf{x} is a vector of commitment-related decisions (e.g., on/off and startup/shutdown) of each generation unit for each time interval over the planning horizon. The continuous variable \mathbf{p} is a vector of each unit dispatch decision for each time interval.

The objective function is to minimize the sum of the commitment cost $\mathbf{b}^\top \mathbf{x}$ (including non-load, startup and shutdown costs) and dispatch cost $\mathbf{c}^\top \mathbf{p}$ over the planning horizon. Constraint (1) involves only commitment-related variables, e.g., minimum up and down times, startup and shutdown constraints, and variable startup costs. Constraint (2) contains dispatch-related constraints, e.g., energy balance (equality can always be written as two opposite inequalities), reserve requirements, transmission limits and ramping constraints. Constraint (3) couples the commitment and dispatch decisions, e.g., minimum and maximum generation capacity constraints. The reader is referred to [11, 14, 16, 18, 19, 21–23, 26] and references therein for further details.

Conventional UC formulations, based on energy scheduling [11, 19, 21, 22, 26], do not represent the unit operation adequately, because they fail to guarantee that the resulting energy schedules can be delivered [10, 15]. To illustrate this problem, consider the following scheduling example for one generating unit. This example assumes that the minimum and maximum generation outputs of the unit are 100 and 300 MW,

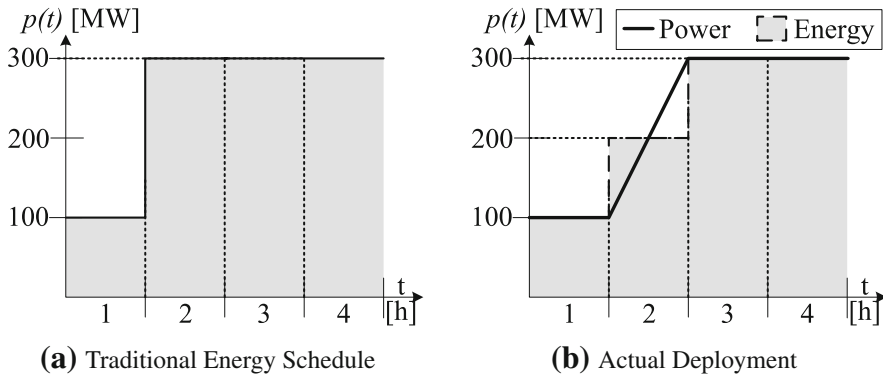


Fig. 1 Scheduling versus deployment

respectively, and that the unit can ramp up from the minimum to the maximum output in 1 h, i.e., 200 MW/h of ramp rate. As shown in Fig. 1a, if the unit has been producing 100 MW during the first hour, then the unit can produce at its maximum output (300 MW) for the next hour. This would be a natural energy schedule resulting from the traditional UC formulations, which are based on the energy scheduling approach. However, the unit is just physically capable of reaching its maximum output before the end of the second hour due to its limited ramp rate, as shown in Fig. 1b. Consequently, the solution obtained in Fig. 1a is not feasible. In fact, the unit requires an infinite ramping capability to be able to reproduce the energy schedule presented in Fig. 1a. More examples about this energy infeasibility problem can be found in [10, 14, 15] and references therein.

Another drawback of conventional UC formulations is that generating units are assumed to start/end their production at their minimum output. That is, their intrinsic startup and shutdown power trajectories are ignored. As a consequence, there is a high amount of energy that is not allocated by UC, but it is inherently present in real time, thus causing a negative economic impact [17] and also demanding a larger quantity of operating reserves to the system [14]. Although some recent works are aware of the importance of including the startup and shutdown processes in UC problems, these power trajectories continue being ignored because the resulting model is considered to largely increase the complexity of the UC problem and hence its computational intensity [3, 8, 13]. For further details of the drawbacks of conventional UC scheduling approaches, the reader is referred to [15, 18] and references therein.

Developing more accurate models would be pointless if they cannot be solved fast enough. Under the mixed integer programming (MIP) approach, it is important to develop tight formulations to reduce the UC computational burden. This allows the implementation of more advanced and computationally demanding problems. A different set of constraints has been proposed to tighten the UC problem [2, 9, 12, 16, 17, 20]. The work in [12, 20] formulates the convex hull of the minimum up and down times. Cuts to tighten ramping limits are presented in [2]. A tighter approximation for quadratic generation costs is proposed [7]. Simultaneously tight and compact MIP formulations for thermal units operation are devised in [9, 16, 17].

To overcome the drawbacks of conventional UC formulations, the model proposed in this paper draws a clear difference between power and energy, and it also takes into account the normally neglected power trajectories that occur during the startup and shutdown processes. Thus, this model adequately represents the operation of generating units to efficiently exploit their flexibility and to avoid infeasible energy delivery. This paper further improves the work in [17] by including the operation of quick-start units and providing the convex hull description for the following set of constraints: generation limits, minimum up and down times, startup and shutdown power trajectories for slow-start units, and startup and shutdown capabilities for quick-start units. Although these convex hulls do not consider some crucial constraints such as ramping, the proposed constraints can be used as the core of any power-based UC formulation, thus tightening the final UC model. In addition, two sets of case studies are carried out: (1) different case studies for a self-UC problem where we only take into account the constraints proposed in this paper, and hence the proposed convex hulls allow solving these self-UC (MIP) instances as linear programs (LP); (2) different case studies for a network-constrained UC problem, where other common constraints are taken into account, such as demand balance, reserves, ramping and transmission limits. These numerical experiments show that the proposed power-based UC formulations solve the MIP problems significantly faster when compared with two other (energy-based) UC formulations commonly known in the literature.

The remainder of this paper is organized as follows. Section 2 introduces the main nomenclature used in this paper. Section 3 details the operating constraints of a single slow- and quick-start unit. In Sect. 4, we provide a convex hull proof for the power-based UC including the constraints mentioned above. Section 5 provides and discusses results from several case studies, where a computational performance comparison with two other traditional UC formulations is made. Finally, some relevant conclusions are drawn in Sect. 6.

2 Nomenclature

Here, we introduce the main notation used in this paper. Lowercase letters are used to denote variables and indexes. Uppercase letters denote parameters.

2.1 Definitions

In this paper, we use the terminology introduced in [17] to refer to the different unit operation states; see Fig. 2.

<i>online</i>	the unit is synchronized with the system.
<i>offline</i>	the unit is not synchronized with the system.
<i>up</i>	the unit is producing above its minimum output. During the <i>up</i> state, the unit output is controllable.
<i>down</i>	the unit is producing below its minimum output: when <i>offline</i> , starting up or shutting down.

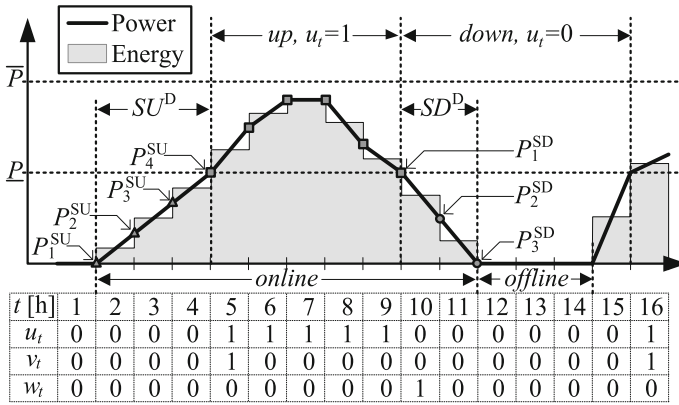


Fig. 2 Operating states including startup and shutdown power trajectories for slow-start units

2.2 Indexes

t Time periods, running from 1 to T hours.

2.3 Unit's technical parameters

- C^{LV} Linear variable cost [\$/MWh].
- C^{NL} No-load cost [\$/h].
- C^{SD} Shutdown cost [\$/].
- C^{SU} Startup cost [\$/].
- \bar{P} Maximum power output [MW].
- \underline{P} Minimum power output [MW].
- P_i^{SD} Power output at the beginning of the i th interval of the shutdown ramp process [MW]; see Fig. 2.
- P_i^{SU} Power output at the beginning of the i th interval of the startup ramp process [MW]; see Fig. 2.
- SD Shutdown capability [MW]; see Fig. 3.
- SU Startup capability [MW]; see Fig. 3.
- SD^D Duration of the shutdown process [h]; see Fig. 2.
- SU^D Duration of the startup process [h]; see Fig. 2.
- TD Minimum down time [h].
- TU Minimum up time [h].

2.4 Continuous decision variables

- e_t Total energy production during period t [MWh].
- p_t Power output at the end of period t , and production above the minimum output \underline{P} [MW].

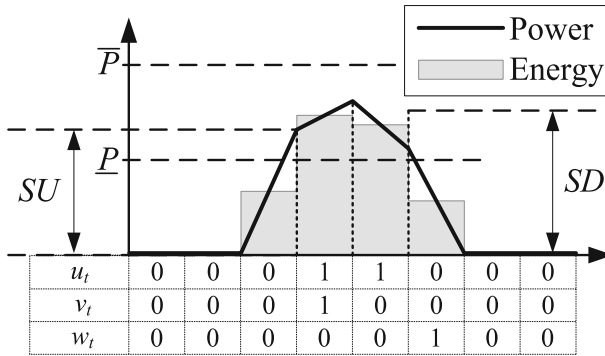


Fig. 3 Startup and shutdown capabilities for quick-start units

\hat{p}_t Total power output at the end of period t , including startup and shutdown power trajectories [MW].

2.5 Binary decision variables

- u_t Commitment status of the unit for period t , which is equal to 1 if the unit is up, and 0 if it is down; see Fig. 2.
- v_t Startup status of the unit, which takes the value of 1 if the unit starts up in period t and 0 otherwise; see Fig. 2.
- w_t Shutdown status of the unit, which takes the value of 1 if the unit shuts down in period t and 0 otherwise; see Fig. 2.

3 Modeling the unit’s operation

The constraints presented here are a further extension of our previous work in [17]. Here, we generalize the formulation by considering quick-start units.

The quick-start units are defined as those that can ramp up from 0 to any value between \underline{P} and SU within one period, typically 1 h, as shown in Fig. 3. Similarly, they can also ramp down from any value between SD and \underline{P} to 0 within one period. On the other hand, the slow-start units are defined as those units that require more than one period to ramp up (down) from 0 (\underline{P}) to \underline{P} (0); see Fig. 2.

The up and down states are distinguished from the online and offline states. Figure 2 shows the different operation states of a thermal unit, as defined in Sect. 2. During the up period ($u_t = 1$), the unit has the flexibility to follow any power trajectory being bounded between the maximum and minimum output. On the other hand, for slow-start units, the power output follows a predefined power trajectory when the unit is starting up or shutting down. The startup and shutdown power trajectories for quick-start units are defined by the startup and shutdown capabilities; see Fig. 3.

This section first presents the basic operating constraints that applies for both slow- and quick-start units. However, the total unit’s production output is different for each

of them. Sections 3.2 and 3.3 show how to obtain the total production, power and energy for slow- and quick-start generating units, respectively.

3.1 Basic operating constraints

The unit’s generation limits taking into account startup SU and shutdown SD capabilities, which are $SU, SD \geq \underline{P}$ by definition, are set as follows; see Fig. 3:

$$p_t \leq (\overline{P} - \underline{P}) u_t - (\overline{P} - SD) w_{t+1} + (SU - \underline{P}) v_{t+1} \quad t \in [1, T - 1] \quad (4)$$

$$p_T \leq (\overline{P} - \underline{P}) u_T \quad (5)$$

$$p_t \geq 0 \quad \forall t \quad (6)$$

and the logical relationship between the decision variables u_t, v_t and w_t ; and the minimum uptime TU and downtime TD limits are ensured with

$$u_t - u_{t-1} = v_t - w_t \quad \forall t \in [2, T] \quad (7)$$

$$\sum_{i=t-TU+1}^t v_i \leq u_t \quad \forall t \in [TU + 1, T] \quad (8)$$

$$\sum_{i=t-TD+1}^t w_i \leq 1 - u_t \quad \forall t \in [TD + 1, T] \quad (9)$$

$$0 \leq u_t \leq 1 \quad \forall t \quad (10)$$

$$0 \leq v_t \leq 1, \quad 0 \leq w_t \leq 1 \quad \forall t \in [2, T], \quad (11)$$

where (7)–(9) describe the convex hull formulation of the minimum up and down time constraints proposed in [20].

3.2 Slow-start units

The slow-start units are assumed to produce \underline{P} at the beginning and at the end of the up state; see Fig. 2. At those points, the startup and shutdown power trajectories are as shown in Fig. 2. Consequently, constraints (4)–(11) describe the operation of slow-start units during the up state when $SU, SD = \underline{P}$.

The minimum down time TD is a function of the minimum offline time, i.e., TD is equal to the startup and shutdown duration processes ($SU^D + SD^D$) plus the minimum offline time of the unit. This then avoids the possible overlapping between the startup and shutdown trajectories. That is, constraint (9) ensures that the unit is down ($u_t = 0$) for enough time to fit the unit’s startup and shutdown power trajectories.

As presented in [17], the total power output including the startup and shutdown power trajectories for slow-start units is obtained with

$$\widehat{p}_t = \underbrace{\underline{P}(u_t + v_{t+1}) + p_t}_{\text{(i) Output when being } up} + \underbrace{\sum_{i=1}^{SU^D} P_i^{SU} v_{t-i+SU^D+2}}_{\text{(iii) SU trajectory}} + \underbrace{\sum_{i=2}^{SD^D+1} P_i^{SD} w_{t-i+2}}_{\text{(ii) SD trajectory}} \quad \forall t. \tag{12}$$

For a better understanding of (12), we can analyze how the power trajectory example in Fig. 2 is obtained from the three different parts in (12):

- (i) Output when the unit is *up*: Although the unit is *up* for five consecutive hours, there are six total power values that are greater than or equal to \underline{P} , from \widehat{p}_4 to \widehat{p}_9 (see the squares in Fig. 2). When $t = 4$, the term v_{t+1} in (i) becomes v_5 ensuring (the first) \underline{P} at the beginning of the *up* period, and the term u_t adds (the remaining five) \underline{P} for $t = 5 \dots 9$. In addition, p_t adds the power production above \underline{P} .
- (ii) Shutdown power trajectory: This process lasts for 2h, $SD^D = 2$; then, the summation term (ii) becomes $P_2^{SD} w_t + P_3^{SD} w_{t-1}$, which is equal to P_2^{SD} for $t = 10$ and P_3^{SD} for $t = 11$, being zero otherwise. This provides the shutdown power trajectory (see the circles in Fig. 2).
- (iii) Startup power trajectory: The startup power trajectory can be obtained using a procedure similar to that used in (ii) (see the triangles in Fig. 2).

Similarly to (12), the total energy production for slow-start units is given by

$$e_t = \underline{P} \cdot u_t + \frac{p_t + p_{t-1}}{2} + \sum_{i=1}^{SD^D} \frac{P_{i+1}^{SD} + P_i^{SD}}{2} w_{t-i+1} + \sum_{i=1}^{SU^D} \frac{P_{i+1}^{SU} + P_i^{SU}}{2} v_{t-i+SU^D+1} \quad \forall t \tag{13}$$

3.3 Quick-start units

The total power for a quick-start unit is given by

$$\widehat{p}_t = \underline{P}(u_t + v_{t+1}) + p_t \quad \forall t \tag{14}$$

and the total energy production is

$$e_t = \frac{\underline{P}(2u_t + v_{t+1} + w_t) + p_{t-1} + p_t}{2} \quad \forall t. \tag{15}$$

It is interesting to note that even though $SU, SD \geq \underline{P}$ (by definition), the resulting energy from (15) may take values below \underline{P} during the startup and shutdown processes; see Fig. 3.

The energy for slow- and quick-start units can also be obtained as a function of the total power output \widehat{p}_t , $e_t = \frac{\widehat{p}_t + \widehat{p}_{t-1}}{2}$ for all t . However sometimes only the total power,

(12) and (14), or the total energy, (13) and (15), production is needed as a function of p, u, v, w .

Notice that (12)–(15) are defined for all t and use variables that are outside the scheduling horizon $[1, T]$. Those variables are considered to be equal to zero when their subindex is $t < 1$ or $t > T$.

In summary, constraints (4)–(11), when $SU, SD = \underline{P}$, together with (12) and (13) describe the technical operation of slow-start units. Constraints (4)–(11) together with (14) and (15) describe the technical operation of quick-start units.

3.4 Total unit operation cost

The objective function of any UC problem involves the total unit operation costs of each generating unit c_t , which is defined as follows:

$$c_t = C^{NL}u_t + C^{LV}e_t + C^{SU'}v_t + C^{SD'}w_t. \tag{16}$$

Note that the no-load cost (C^{NL}) considered in (16) ignores the startup and shutdown periods. This is because the C^{NL} only multiplies the commitment during the up state u_t . To consider the no-load cost during the startup and shutdown periods, $C^{SU'}$ and $C^{SD'}$ are introduced in (16) and defined as:

$$C^{SU'} = C^{SU} + C^{NL}SU^D \tag{16a}$$

$$C^{SD'} = C^{SD} + C^{NL}SD^D, \tag{16b}$$

where $SU^D, SD^D = 1$ for quick-start units; see Fig. 3.

4 Convex hull proof

In this section, we first prove that inequalities (4)–(6) are facet defining and then that inequalities (4)–(11) define an integral polytope. Finally, we also prove that inequalities describing the operation of slow-start units, (4)–(11) together with equalities (12)–(13), define an integral polytope. Similarly, inequalities describing the operation of quick-start units, (4)–(11) together with equalities (14)–(15), also define an integral polytope.

Note that the variables w_t are completely determined in terms of u_t and v_t using (7). Therefore, in the following we eliminate variables w_t and assume that constraints (4), (9), and (11) are reformulated accordingly.

Definition 1 Let $\overline{D}_T(TU, TD, \overline{P}, \underline{P}, SU, SD) = \{(u, v, p) \in \mathbb{R}_+^{3T-1} \mid (u, v, p) \text{ satisfy (4)–(11)}\}$. Let $\overline{C}_T(TU, TD, \overline{P}, \underline{P}, SU, SD)$ be the convex hull of the points in $\overline{D}_T(TU, TD, \overline{P}, \underline{P}, SU, SD)$ such that $u \in \{0, 1\}^T, v \in \{0, 1\}^{T-1}$.

For short, we denote $\overline{C}_T(TU, TD, \overline{P}, \underline{P}, SU, SD)$ by \overline{C}_T and $\overline{D}_T(TU, TD, \overline{P}, \underline{P}, SU, SD)$ by \overline{D}_T .

	u_1	u_2	\dots	u_{t-1}	u_t	u_{t+1}	\dots	u_{T-1}	u_T	p_1	\dots	p_{t-1}	p_t	\dots	p_{T-1}	p_T	v_2	\dots	v_{t-1}	v_t	u_{t+1}	\dots	v_{T-1}	v_T	w_2	\dots	w_{t-1}	w_t	w_{t+1}	\dots	w_{T-1}	w_T
$x^{(1)}$	1	0	\dots	0	0	0	\dots	0	0	0	\dots	0	0	\dots	0	0	0	\dots	0	0	0	\dots	0	0	1	\dots	0	0	0	\dots	0	0
$x^{(2)}$	1	1	\dots	0	0	0	\dots	0	0	0	\dots	0	0	\dots	0	0	0	\dots	0	0	0	\dots	0	0	0	\dots	0	0	0	\dots	0	0
\vdots	\vdots	\vdots	\dots	\vdots	\vdots	\vdots	\dots	\vdots	\vdots	\vdots	\dots	\vdots	\vdots	\dots	\vdots	\vdots	\vdots	\dots	\vdots	\vdots	\dots	\vdots	\vdots	\vdots	\dots	\vdots	\vdots	\vdots	\vdots	\vdots	\vdots	
$x^{(t-1)}$	1	1	\dots	1	0	0	\dots	0	0	0	\dots	0	0	\dots	0	0	0	\dots	0	0	0	\dots	0	0	0	\dots	0	1	0	\dots	0	0
$x^{(t)}$	1	1	\dots	1	1	0	\dots	0	0	0	\dots	0	0	\dots	0	0	0	\dots	0	0	0	\dots	0	0	0	\dots	0	1	0	\dots	0	0
$x^{(t+1)}$	1	1	\dots	1	1	1	\dots	0	0	0	\dots	0	g_t	\dots	0	0	0	\dots	0	0	0	\dots	0	0	0	\dots	0	0	0	\dots	0	0
\vdots	\vdots	\vdots	\dots	\vdots	\vdots	\vdots	\dots	\vdots	\vdots	\vdots	\dots	\vdots	\vdots	\dots	\vdots	\vdots	\vdots	\dots	\vdots	\vdots	\dots	\vdots	\vdots	\vdots	\dots	\vdots	\vdots	\vdots	\vdots	\vdots	\vdots	
$x^{(T-1)}$	1	1	\dots	1	1	1	\dots	1	0	0	\dots	0	g_t	\dots	0	0	0	\dots	0	0	0	\dots	0	0	0	\dots	0	0	0	\dots	0	1
$x^{(T)}$	1	1	\dots	1	1	1	\dots	1	1	0	\dots	0	g_t	\dots	0	g^T	0	\dots	0	0	0	\dots	0	0	0	\dots	0	0	0	\dots	0	0
$y^{(1)}$	1	0	\dots	0	0	0	\dots	0	0	D	\dots	0	0	\dots	0	0	0	\dots	0	0	0	\dots	0	0	1	\dots	0	0	0	\dots	0	0
$y^{(2)}$	1	1	\dots	0	0	0	\dots	0	0	P	\dots	D	0	\dots	0	0	0	\dots	0	0	0	\dots	0	0	0	\dots	0	0	0	\dots	0	0
\vdots	\vdots	\vdots	\dots	\vdots	\vdots	\vdots	\dots	\vdots	\vdots	\vdots	\dots	\vdots	\vdots	\dots	\vdots	\vdots	\vdots	\dots	\vdots	\vdots	\dots	\vdots	\vdots	\vdots	\dots	\vdots	\vdots	\vdots	\vdots	\vdots	\vdots	
$y^{(t-1)}$	1	1	\dots	1	0	0	\dots	0	0	\hat{P}	\dots	\hat{D}	0	\dots	0	0	0	\dots	0	0	0	\dots	0	0	0	\dots	0	1	0	\dots	0	0
$y^{(t)}$	1	1	\dots	1	1	0	\dots	0	0	P	\dots	P	D	\dots	0	0	0	\dots	0	0	0	\dots	0	0	0	\dots	0	1	0	\dots	0	0
$y^{(t+1)}$	1	1	\dots	1	1	1	\dots	0	0	P	\dots	P	P	\dots	0	0	0	\dots	0	0	0	\dots	0	0	0	\dots	0	0	0	\dots	0	0
\vdots	\vdots	\vdots	\dots	\vdots	\vdots	\vdots	\dots	\vdots	\vdots	\vdots	\dots	\vdots	\vdots	\dots	\vdots	\vdots	\vdots	\dots	\vdots	\vdots	\dots	\vdots	\vdots	\vdots	\dots	\vdots	\vdots	\vdots	\vdots	\vdots	\vdots	
$y^{(T-1)}$	1	1	\dots	1	1	1	\dots	1	0	\hat{P}	\dots	\hat{P}	\hat{P}	\dots	0	0	0	\dots	0	0	0	\dots	0	0	0	\dots	0	0	0	\dots	0	1
$y^{(T)}$	1	1	\dots	1	1	1	\dots	1	1	P	\dots	P	P	\dots	0	0	0	\dots	0	0	0	\dots	0	0	0	\dots	0	0	0	\dots	0	0
$z^{(1)}$	0	1	\dots	1	1	1	\dots	1	1	U	\dots	0	g_t	\dots	0	g^T	1	\dots	0	0	0	\dots	0	0	0	\dots	0	0	0	\dots	0	0
$z^{(2)}$	0	0	\dots	1	1	1	\dots	1	1	0	\dots	0	g_t	\dots	0	g^T	0	\dots	0	0	0	\dots	0	0	0	\dots	0	0	0	\dots	0	0
\vdots	\vdots	\vdots	\dots	\vdots	\vdots	\vdots	\dots	\vdots	\vdots	\vdots	\dots	\vdots	\vdots	\dots	\vdots	\vdots	\vdots	\dots	\vdots	\vdots	\dots	\vdots	\vdots	\vdots	\dots	\vdots	\vdots	\vdots	\vdots	\vdots	\vdots	
$z^{(t-2)}$	0	0	\dots	0	1	1	\dots	1	1	0	\dots	0	g_t	\dots	0	g^T	0	\dots	0	0	0	\dots	0	0	0	\dots	0	0	0	\dots	0	0
$z^{(t-1)}$	0	0	\dots	0	1	1	\dots	1	1	0	\dots	0	g_t	\dots	0	g^T	0	\dots	0	1	0	\dots	0	0	0	\dots	0	0	0	\dots	0	0
$z^{(t)}$	0	0	\dots	0	0	0	\dots	1	1	0	\dots	0	0	\dots	0	g^T	0	\dots	0	0	0	\dots	0	0	0	\dots	0	0	0	\dots	0	0
\vdots	\vdots	\vdots	\dots	\vdots	\vdots	\vdots	\dots	\vdots	\vdots	\vdots	\dots	\vdots	\vdots	\dots	\vdots	\vdots	\vdots	\dots	\vdots	\vdots	\dots	\vdots	\vdots	\vdots	\dots	\vdots	\vdots	\vdots	\vdots	\vdots	\vdots	
$z^{(T-1)}$	0	0	\dots	0	0	0	\dots	0	1	0	\dots	0	0	\dots	0	U	g^T	\dots	0	0	0	\dots	0	1	0	\dots	0	0	0	\dots	0	0
$z^{(T)}$	0	0	\dots	0	0	0	\dots	0	0	0	\dots	0	0	\dots	0	0	0	\dots	0	0	0	\dots	0	0	0	\dots	0	0	0	\dots	0	0
$y^{(T+1)}$	1	1	\dots	1	1	1	\dots	1	1	P	\dots	P	P	\dots	0	0	0	\dots	0	0	0	\dots	0	0	0	\dots	0	0	0	\dots	0	0

Fig. 4 $3T$ Affinely independent points for $g_t, g^T = 0, g_t^y = P$ and $g_t^z = U$, where $U = SU - P, D = SD - P$ and $P = \bar{P} - P$

To facilitate the proofs, we introduce the points $x^i, y^i, z^i \in \bar{C}_T$, as shown in Fig. 4. We also introduce the parameters U, D and P which are equivalent to $U = SU - P, D = SD - P$ and $P = \bar{P} - P$, respectively.

Proposition 1 \bar{C}_T is full dimensional in terms of u, v and p .

Proof From Fig. 4, it can be easily shown that the $3T$ points x^i, y^i and z^i for $i \in [1, T]$ are affinely independent when $g_t, g^T = 0, g_t^y = P$ and $g_t^z = U$. Note that in case $D = 0$, the point $y^{(1)}$ must be removed and the point $y^{(T+1)}$ added, thus keeping the $3T$ affinely independent points. This applies for all the following proofs; but for the sake of brevity, we assume from now on that $D \neq 0$. \square

Theorem 1 The inequalities in (4) describe facets of the polytope \bar{C}_T .

Proof We show that (4) describe facets of \bar{C}_T by the direct method [25]. We do so by presenting $3T - 1$ affinely independent points in \bar{C}_T that are tight (satisfying as an equality) for the given inequality. Note in Fig. 4 that the point z^T (the origin) satisfies (4)–(6) as equality. Therefore, to get $3T - 1$ affinely independent points, we need only $3T - 2$ other linearly independent points.

The following $3T - 2$ points are linearly independent and tight for (4) when $g^T = 0, g_t, g_t^y = P$ and $g_t^z = U$: $T - 1$ points x^i for $i \in [1, t - 1] \cup [t + 1, T]$, T points y^i for $i \in [1, T]$, and $T - 1$ points z^i for $i \in [1, T - 1]$. \square

Theorem 2 The inequality (5) describes a facet of the polytope \bar{C}_T .

Proof As mentioned before, it suffices to show $3T - 2$ linearly independent points that are tight for (5). The following $3T - 2$ points are linearly independent and tight for (5) when $g_t = 0, g^T, g_t^y = P$ and $g_t^z = U$: T points x^i for $i \in [1, T]$, $T - 1$ points y^i for $i \in [1, T - 1]$, and $T - 1$ points z^i for $i \in [1, T - 1]$. \square

Theorem 3 *The inequalities in (6) describe facets of the polytope \overline{C}_T .*

Proof The following $3T - 2$ points are linearly independent and tight for (6) when $g_t, g_t^y, g_t^z, g^T = 0$: T points x^i for $i \in [1, T]$, $T - 1$ points y^i for $i \in [1, t - 1] \cup [t + 1, T]$, and $T - 1$ points z^i for $i \in [1, T - 1]$. \square

We may conclude that (4)–(6) describe facets of \overline{C}_T .

Now, we prove that the inequalities (4)–(11) are sufficient to describe the convex hull of the feasible solutions.

We need a preliminary lemma.

Lemma 1 *Let $P = \{x \in \mathbb{R}^n | Ax \leq b\}$ be an integral polyhedron, i.e., $P = \text{conv}(P \cap \mathbb{Z}^n)$. Define $Q = \{(x, y) \in \mathbb{R}^n \times \mathbb{R}^m | x \in P, 0 \leq y_i \leq c_i x, i = 1, \dots, k, y_i = d_i x, i = k + 1, \dots, m\}$, where $1 \leq k \leq m, c_i, d_i \in \mathbb{R}^n$, and $c_i x \geq 0, d_i x \geq 0$ for $i = 1, \dots, m$ and for each $x \in P$. Then every vertex (\tilde{x}, \tilde{y}) of Q has the property that \tilde{x} is integral.*

Proof Suppose by contradiction that there exists a vertex (\tilde{x}, \tilde{y}) of Q , such that \tilde{x} is not integral. Then, \tilde{x} is not a vertex of P and therefore there exist $\tilde{x}^1, \tilde{x}^2 \in P$, such that $\tilde{x} = \frac{1}{2}\tilde{x}^1 + \frac{1}{2}\tilde{x}^2$. Moreover, $\tilde{y}_i = c_i \tilde{x}$ for $i = 1, \dots, k$; indeed, if there exists $r, 1 \leq r \leq k$, such that $0 \leq \tilde{y}_r < c_r \tilde{x}$, then (\tilde{x}, \tilde{y}) is a convex combination of the point (\tilde{x}, \hat{y}) and the point (\tilde{x}, \check{y}) , where $\hat{y}_r = c_r \tilde{x}, \check{y}_r = 0$, and $\hat{y}_i = \check{y}_i = \tilde{y}_i$ for $1 \leq i \leq m, i \neq r$.

For $j = 1, 2$, let $\tilde{y}_i^j = c_i \tilde{x}^j$ for $i = 1, \dots, k$ and $\tilde{y}_i^j = d_i \tilde{x}^j$ for $i = k + 1, \dots, m$. Then $(\tilde{x}, \tilde{y}) = \frac{1}{2}(\tilde{x}^1, \tilde{y}^1) + \frac{1}{2}(\tilde{x}^2, \tilde{y}^2)$, i.e., (\tilde{x}, \tilde{y}) is a convex combination of $(\tilde{x}^1, \tilde{y}^1)$ and $(\tilde{x}^2, \tilde{y}^2)$. Contradiction. \square

Theorem 4 *The polytopes \overline{C}_T and \overline{D}_T are equal.*

Proof The thesis can be proved by showing that \overline{D}_T defines an integral polytope. This easily follows by applying Lemma 1, considering P as the integer polytope defined by inequalities (8)–(11) (see [20]), p_t as the additional variables and (4)–(6) as the new inequalities.

Finally, we prove that inequalities describing the operation of slow- and quick-start units to define integral polytopes. \square

Definition 2 Let the polytope that describes the operation of slow-start units be $\overline{S}_T(\text{TU}, \text{TD}, \overline{P}, \underline{P}, \text{SU}^D, \text{SD}^D, P_i^{\text{SU}}, P_i^{\text{SD}}) = \{(u, v, p, \hat{p}, e) \in \mathbb{R}_+^{5T-1} | (u, v, p)$ satisfying inequalities (4)–(13) for $\text{SU}, \text{SD} = \underline{P}\}$, for short denoted as \overline{S}_T . Let the polytope that describes the operation of quick-start units be $\overline{Q}_T(\text{TU}, \text{TD}, \overline{P}, \underline{P}, \text{SU}, \text{SD},) = \{(u, v, p, \hat{p}, e) \in \mathbb{R}_+^{5T-1} | (u, v, p)$ satisfying inequalities (4)–(11) and (14)–(15)\}, for short denoted as \overline{Q}_T .

Theorem 5 *The polytopes \overline{S}_T and \overline{Q}_T define integer polytopes on variables u, v .*

Proof This easily follows by applying Lemma 1. For the polytope describing the operation of slow-start units \overline{S}_T , P is the integer polytope \overline{D}_T (see Theorem 4), \hat{p}_t, e_t are the additional variables, and (12)–(13) the new equalities. Similarly, for the polytope describing the operation of quick-start units \overline{Q}_T , P is the integer polytope \overline{D}_T , \hat{p}_t, e_t are the additional variables, and (14)–(15) the new equalities. \square

Concluding, the constraints describing the technical operation of both slow- and quick-start units are convex hulls. These constraints are (4)–(11), when SU, SD = \underline{P} , together with (12) and (13) for slow-start units; and (4)–(11) together with (14) and (15) for quick-start units.

In short, the entire formulation (4)–(15) defines an integral polytope.

5 Numerical results

To illustrate the computational performance of the formulation proposed in this paper, two sets of case studies are carried out: one for a self-UC problem and another for a network-constrained UC problem. This section compares the computational performance of the proposed power-based formulation with two energy-based formulations, [1] and [4], which have been recognized as computationally efficient in the literature [14, 18, 23].

The following three formulations are then implemented:

- *Pw*: This is the complete formulation proposed in this paper. For the network-constrained UC, we include other common constraints such as demand balance, reserves, ramping and transmission limits. The complete network-constrained power-based UC is presented in Appendix .
- *1bin*: This formulation is presented in [1] and requires a single set of binary variables (per unit and per period), i.e., the startup and shutdown decisions are expressed as a function of the commitment decision variables.
- *3bin*: The convex hull of the minimum up/down time constraints proposed in [20] [see (8) and (9)] are implemented with the three-binary equivalent formulation of *1bin*. This formulation is presented in [4].

Notice that a different set of constraints is used for the self-UC and for the network-constrained UC problems. For the self-UC problems, *1bin* and *3bin* are modeled only considering (1) generation limits, (2) minimum up and down times, and (3) startup and shutdown capabilities: the same set of constraints presented in Sect. 3. For the network-constrained UC problems, *1bin* and *3bin* are modeled taking into account the full set of constraints presented in [1] and its 3-bin equivalent [4], respectively; in addition, these formulations are further extended by introducing downward reserve (which is modeled in the same fashion as the upward reserve; see [1, 14, 16]), transmission limits [see (22) in Appendix] and wind generation [which is taken into account in the demand balance (19) and transmission-limit constraints (22)].

It is important to highlight that the energy-based UC formulations *1bin* and *3bin* represent the same mixed-integer optimization problem. The difference between them is how the constraints are formulated. In other words, for a given case study, *1bin* and *3bin* obtain the same optimal results, e.g., commitments, generating outputs and operation costs. On the other hand, the power-based formulation obtains different optimal results, since the constraints are based on power-production variables rather than energy-output variables. The reader is referred to [14, 18] for further and detailed discussions about the differences between the optimal power-based and energy-based scheduling.

Table 1 Generator data for quick-start units

Gen	Technical information							Cost coefficients [†]			
	\bar{P} (MW)	P (MW)	TU and TD (h)	SU (MW)	SD (MW)	p_0^* (MW)	Ste_0^\diamond (h)	C^{NL} (\$/h)	C^{LV} (\$/MWh)	C^{SU} (\$)	C^{SD} (\$)
1	455	150	8	252	303	150	8	1000	16.19	9000	0
2	455	150	8	252	303	150	8	970	17.26	10,000	0
3	130	20	5	57	75	20	5	700	16.60	1100	0
4	130	20	5	57	75	20	5	680	16.50	1120	0
5	162	25	6	71	94	25	6	450	19.70	1800	0
6	80	20	3	40	50	20	3	370	22.26	340	0
7	85	25	3	45	55	25	3	480	27.74	520	0
8	55	10	1	25	33	10	1	660	25.92	60	0
9	55	10	1	25	33	10	1	665	27.74	60	0
10	55	10	1	25	33	10	1	670	27.79	60	0

* p_0 is the unit’s initial production prior to the first period of the time span

◊ Ste_0 : hours that the unit has been online prior to the first period of the time span

All tests were carried out using CPLEX 12.5 on an Intel-i7 3.4-GHz personal computer with 8 GB of RAM memory. The problems are solved until they hit the time limit of 10,000 s or until they reach optimality (more precisely to 10^{-6} of relative optimality gap).

5.1 Self-UC

Here, a self-UC problem for a price-taker producer is solved for different time spans. The goal is then to optimally schedule the generating units to maximize profits (difference between the revenue and the total operating cost [5, 17]) during the planning horizon:

$$\max \sum_{t=1}^N \sum_{g=1}^G [\pi_t e_{gt} - c_{gt}(u_{gt}, v_{gt}, w_{gt}, e_{gt})] \tag{17}$$

where subindex g stands for generating units and G is the total quantity of units; π_t refers to the energy prices, which for these case studies are shown in Table 2; and c_{gt} is the total operating cost per unit g at period t , which is defined in (16) for the proposed power-based UC formulation. The self-UC problem also arises when solving UC with decomposition methods such as Lagrangian relaxation [6].

Two different ten-unit system data are considered, one containing only quick-start units and another containing both quick- and slow-start units. The ten-unit system data for quick-start units are presented in Table 1. The power system data are based on information presented in [1, 16]. For this system of ten quick-start units, we also include a power-based formulation that only models quick-start units (see Sect. 3), labeled as PwQ .

Table 2 Energy price (\$/MWh)

$t = 1 \dots 12 \rightarrow$	13.0	7.2	4.6	3.3	3.9	5.9	9.8	15.0	22.1	31.3	33.2	24.8
$t = 13 \dots 24 \rightarrow$	19.5	16.3	14.3	13.7	15.0	17.6	20.2	29.3	49.5	53.4	30.0	20.2

Table 3 Generator data for slow-start units

Gen	Technical information								
	\bar{P} (MW)	\underline{P} (MW)	TU and TD (h)	SU (MW)	SD (MW)	SU ^D (h)	SD ^D (h)	p_0 (MW)	Ste ₀ (h)
1	455	150	8	150	150	3	2	150	8
2	455	150	8	150	150	3	2	150	8
3	130	20	5	20	20	2	2	20	5
4	130	20	5	20	20	2	2	20	5
5	162	25	6	25	25	2	2	25	6
6	80	20	3	20	20	1	1	20	3
7	85	25	3	25	25	1	1	25	3

Another 10-unit system data set including slow-start units is created to observe the computational performance of the formulation for slow-start units. We create this new case study by replacing the first seven quick-start units from Table 1 by slow-start units. The data for these seven slow-start units are provided in Table 3. For these slow-start units, the power outputs for the startup (shutdown) power trajectories are obtained as an hourly linear change from 0 (\underline{P}) to \bar{P} (0) for a duration of SU^D (SD^D) hours. *1bin* and *3bin* are modeled only for quick-start units because: (1) those traditional UC formulations ignore the units’ startup and shutdown power trajectories and including these trajectories will considerably increase the models’ computing complexity [17]; and (2) the main purpose of these case studies is to compare the computational performance of the proposed formulations with the traditional UC formulations (which ignore the startup and shutdown trajectories).

In short, two different case studies are carried out for the self-UC problem, the first case study models ten quick-start units (see Table 1) for formulations *3bin*, *1bin* and *PwQ*. The second case study also models ten units, seven slow-start (see Table 3) and three quick-start units (units 8 to 10 in Table 1). This case study is solved using the proposed power-based formulation for both slow- and quick-start units, which is labeled as *Pw*.

Table 4 shows the computational performance of the self-UC problem (17) subject to the different UC formulations for different time spans (up to 512 days to consider large case studies). The tightness of each formulation is measured with the integrality gap (IntGap) and the integrality gap in the root node (RootIGap). The IntGap is defined as the relative distance between the MIP and LP optima [16,24], where the MIP optimum corresponds to the best integer solution that could be found, and the LP optimum corresponds to the LP relaxation of the MIP formulation. The RootIGap is obtained as the relative difference between the upper and lower bounds

Table 4 Computational performance of the UC formulations for different time spans (in days)

Days	IntGap (%)			RootIGap (%)			LP time (s)			MIP time (s)*		B&B nodes			
	<i>Pw</i> [◇]	<i>3bin</i>	<i>1bin</i>	<i>Pw</i> [◇]	<i>3bin</i>	<i>1bin</i>	<i>PwQ</i> [†]	<i>Pw</i> [†]	<i>3bin</i>	<i>1bin</i>	<i>3bin</i>	<i>1bin</i>	<i>Pw</i> [◇]	<i>3bin</i>	<i>1bin</i>
64	0	0.88	2.57	0	0.027	0.063	0.42	0.47	0.80	0.95	12.01	13.79	0	496	487
128	0	0.87	2.57	0	0.026	0.050	1.03	1.22	2.06	2.60	45.54	(0.033)	0	528	603915
256	0	0.87	2.57	0	0.026	0.058	2.62	3.15	5.38	6.88	199.18	(0.052)	0	533	229035
512	0	0.87	2.57	0	0.026	0.056	6.96	8.55	14.29	18.83	734.03	(0.054)	0	488	136128

* (·) shows the final optimality gap in % if the time limit is reached

◇ *PwQ* is equal to *Pw* for these cases

† For these formulations, the LP and MIP times are equal

Table 5 Problem size comparison of the UC formulations for different time spans (in days)

Days	# constraints			# nonzero elements				# real var			# binary var		
	<i>Pw</i> [*]	<i>3bin</i>	<i>1bin</i>	<i>PwQ</i>	<i>Pw</i>	<i>3bin</i>	<i>1bin</i>	<i>Pw</i> [*]	<i>3bin</i>	<i>1bin</i>	<i>Pw</i> [*]	<i>3bin</i>	<i>1bin</i>
64	76749	107459	138225	432673	440339	417313	469719	30720	15360	46080	46080	46080	15360
128	153549	214979	276465	865825	881171	835105	939735	61440	30720	92160	92160	92160	30720
256	307149	430019	552945	1732129	1762835	1670689	1879767	122880	61440	184320	184320	184320	61440
512	614349	860099	1105905	3464737	3526163	3341857	3759831	245760	122880	368640	368640	368640	122880

^a *PwQ* is equal to *Pw* for these cases

before the branching process (after the solver applies initial cuts and heuristics at the root node). Beware that the IntGap of two formulations which are not modeling exactly the same problem should not be directly compared. Therefore, IntGap together with RootIGap provide a better indication of the strength of each formulation.

Note that the MIP optima of *PwQ* and *Pw* were achieved by just solving the LP problem, IntGap = 0 (thus RootIGap = 0), hence solving the MIP problems in LP time. On the other hand, as usual, the branch-and-cut method was needed to solve the MIP for *3bin* and *1bin*. Table 4 also shows the MIP time and the branch-and-bound nodes (B&B nodes) that were explored for the different formulations.

Table 5 shows the dimensions for all formulations for the different time spans. Note that *PwQ* and *Pw* are more compact, in terms of quantity of constraints, than *3bin* and *1bin*. The formulations *PwQ* and *Pw* present the same quantity of binary variables of *3bin*, but twice continuous variables. This is because *PwQ* and *Pw* model power and energy as two different variables. The formulation *1bin* presents a third of binary variables in comparison with the other formulations, but it is the formulation presenting the largest quantity of continuous variables, constraints and nonzero elements in the constraint matrix. This is the result of reformulating the MIP model to avoid the startup and shutdown binary variables. The work in [1] claims that this would reduce the node enumeration in the branch-and-bound process. Note however that this reformulation is the least tight, see IntGap and RootIGap in Table 4, and it is also the largest, hence presenting the worst computational performance; similar results are obtained in [16].

Table 6 IEEE 118-bus system results: computational performance of the UC formulations for different time spans (in hours)

Hours	IntGap (%)			RootIGap (%)			LP time (s)			MIP time (s)*			B&B Nodes		
	<i>Pw</i>	<i>3bin</i>	<i>1bin</i>	<i>Pw</i>	<i>3bin</i>	<i>1bin</i>	<i>Pw</i>	<i>3bin</i>	<i>1bin</i>	<i>Pw</i>	<i>3bin</i>	<i>1bin</i>	<i>Pw</i>	<i>3bin</i>	<i>1bin</i>
24	0.89	1.13	1.75	0.089	0.375	1.052	0.44	2.48	2.9	27.61	585.22	(0.094)	1581	93285	889610
36	1.46	0.98	1.87	0.031	0.393	1.050	1.12	10.28	13.56	34.54	(0.103)	(0.179)	1189	534480	137325
48	1.06	0.7	1.37	0.027	0.504	0.943	1.7	17.87	19.19	69.58	(0.095)	(0.269)	1673	260545	40115
60	1.37	0.71	1.54	0.034	0.484	0.828	3.53	37.89	40.86	267.23	(0.148)	(0.326)	1982	146818	26718

* (-) shows the final optimality gap in % if the time limit is reached

5.2 Network-constrained UC

Here, the modified IEEE 118-bus test system is used for different time spans, from 24 to 60h. All system data can be found in [14]. The IEEE-118 bus system has 118 buses; 186 transmission lines; 54 thermal units (both quick- and slow-start units); 91 loads, with average and maximum levels of 3991 MW and 5592 MW, respectively; and three wind units, with aggregated average and maximum production of 867 MW and 1333 MW, respectively, for the nominal wind case. Finally, the upward and downward reserve requirement are set as the 5% of the total nominal wind production for each hour. The network-constrained UC problem is considerably more complex than the self-UC problem described in Sect. 5.1, due to the new complicating constraints that are now included (into all the formulations), such as demand balance, reserves, ramping and transmission limits (see Appendix).

Table 6 shows the computational performance of the network-constrained UC problem for all formulations and different time spans (up to 60 h). On the one hand, the IntGap of *Pw* is always lower than that of *1bin*, but higher than that of *3bin*. However, as mentioned above, the IntGap of *Pw* and *3Bin* (or *1bin*) cannot be compared directly because they do not represent the same problem (*3bin* and *1bin* which are equivalent, thus providing the same optimal results). Hence, based on the IntGap, *3bin* seems the tightest formulation. On the other hand, based on the RootIGap, *Pw* seems the tightest, up to 18x and 35x tighter than *3bin* a *1bin*, respectively. Notice that *Pw* was the only formulation that solved all the cases within the time limit (10,000s), *3bin* could only solve the smallest case and *1bin* none of them. For the cases where *3bin* and *1bin* could not be solved (time spans equal and above 36 h), *Pw* could achieve a lower initial optimality gap (RootIGap) than the final optimality gap achieved by *3bin* and *1bin* (in 10,000 s). Furthermore, *Pw* could achieve this initial optimality gap in a few seconds: 3.82, 10.14, 16.80, 27.87s for the cases with time spans of 24, 36, 48 and 60h, respectively. These times are similar to (and even lower than) the times required by *1bin* and *3bin* to solve their LP relaxation. We can then conclude that *Pw* is the tightest formulation due to its superiority in solving the MIP problems.

Table 5 shows the problem size for all formulations for different time spans. Similarly to the self-UC case study (Sect. 5.1), *Pw* is more compact than the others, in terms of quantity of constraints and nonzeros, but *Pw* has more continuous variables. Also, although *1bin* has a third of binary variables in comparison with the others, it has the largest quantity of constraints and it is the least tight (see IntGap and RootIGap

Table 7 IEEE 118-bus system results: problem size comparison of the UC formulations for different time spans (in hours)

Hours	# constraints			# nonzero elements			# real var			# binary var		
	Pw^*	$3bin$	$1bin$	Pw	$3bin$	$1bin$	Pw^*	$3bin$	$1bin$	Pw^*	$3bin$	$1bin$
64	18093	37803	38141	315424	473791	472969	13518	9720	11016	3888	3888	1296
128	27489	56919	57257	476404	734431	732457	20322	14580	16524	5832	5832	1944
256	36885	76035	76373	637384	995071	991945	27126	19440	22032	7776	7776	2592
512	46281	95151	95489	798364	1255711	1251433	33930	24300	27540	9720	9720	3240

* PwQ is equal to Pw for these cases

in Table 4), consequently presenting the worst computational performance, as also discussed in Sect. 5.1.

In conclusion, from both self-UC and network-constrained UC case studies, the proposed formulation presented a dramatic improvement in computation in comparison with $3bin$ and $1bin$ due to its tightness (speedups above 85x and 8200x, respectively) and it also presents a lower LP burden due to its compactness (see Table 5 and Table 7).

6 Conclusion

This paper presented the convex hull description of the basic constraints of slow- and quick-start generating units for power-based unit commitment (UC) problems. These constraints are: generation limits, and minimum up and down times, startup and shutdown power trajectories for slow-start units, and startup and shutdown capabilities for quick-start units. Although the model does not include some crucial constraints, such as ramping, it can be used as the core of any UC formulation and thus help to tighten the final UC model. Finally, two different sets of case studies were carried out, for a self-UC and for a network-constrained UC, where the proposed formulation was simultaneously tighter and more compact when compared with two other UC formulations commonly known in the literature, consequently, solving both UC problems significantly faster.

Acknowledgments The authors thank Laurence Wolsey, Santanu Dey and Paolo Ventura for useful discussions about the proof of the Lemma 1. **Compliance with Ethics Requirements** The authors declare that they have no conflict of interest. This article does not contain any studies with human or animal subjects.

Open Access This article is distributed under the terms of the Creative Commons Attribution 4.0 International License (<http://creativecommons.org/licenses/by/4.0/>), which permits unrestricted use, distribution, and reproduction in any medium, provided you give appropriate credit to the original author(s) and the source, provide a link to the Creative Commons license, and indicate if changes were made.

Appendix: Network-constrained power-based UC formulation

Here, we present the network-constrained power-based UC formulation, the core of which is based on the constraints presented in Sect. 3. Although some nomenclature

and constraints were introduced before, for the sake of clarity and completeness, this section provides the complete nomenclature and set of constraints.

Nomenclature

Indexes and sets

$g \in \mathcal{G}$	Generating units, running from 1 to G .
\mathcal{G}^Q	Set of quick-start generating units in \mathcal{G} .
\mathcal{G}^S	Set of slow-start generating units in \mathcal{G} .
$b \in \mathcal{B}$	Buses, running from 1 to B .
$l \in \mathcal{L}$	Transmission lines, running from 1 to L .
$t \in \mathcal{T}$	Hourly periods, running from 1 to T hours.

System parameters

D_{bt}	Power demand on bus b at the end of hour t [MW].
D_t^-	System requirements for downward reserve for hour t [MW].
D_t^+	System requirements for upward reserve for hour t [MW].
\overline{F}_l	Power flow limit on transmission line l [MW].
Γ_{lb}	Shift factor for line l associated with bus b [p.u.].
Γ_{lg}^G	Shift factor for line l associated with unit g [p.u.].
P_{bt}^W	Nominal forecasted wind power at the end of hour t [MW].

Unit's parameters

C_g^{LV}	Linear variable production cost [\$/MWh].
C_g^{NL}	No-load cost [\$/h].
C_g^{SD}	Shutdown cost [\$/].
C_g^{SU}	Startup cost [\$/].
\overline{P}_g	Maximum power output [MW].
\underline{P}_g	Minimum power output [MW].
P_{gi}^{SD}	Power output at the beginning of the i^{th} interval of the shutdown ramp process [MW].
P_{gi}^{SU}	Power output at the beginning of the i^{th} interval of the startup ramp process [MW].
RD_g	Ramp-down capability [MW/h].
RU_g	Ramp-up capability [MW/h].
SD_g	Shutdown capability [MW].
SU_g	Startup capability [MW].
SD_g^D	Duration of the shutdown process [h].
SU_g^D	Duration of the startup process [h].
TD_g	Minimum down time [h].
TU_g	Minimum up time [h].

Decision variables

p_{bt}^W	Wind power output at the end of hour t [MW].
e_{gt}	Total energy output during hour t [MWh].
p_{gt}	Power output above minimum output at the end of hour t [MW].
\widehat{p}_{gt}	Total power output at the end of hour t , including startup and shutdown power trajectories [MW].
r_{gt}^-	Downward capacity reserve [MW].
r_{gt}^+	Upward capacity reserve [MW].
u_{gt}	Binary variable which is equal to 1 if the unit is producing above minimum output and 0 otherwise.
v_{gt}	Binary variable which takes the value of 1 if the unit starts up and 0 otherwise.
w_{gt}	Binary variable which takes the value of 1 if the unit shuts down and 0 otherwise.

Objective function

The UC seeks to minimize all production costs (Sect. 1):

$$\min \sum_{g \in \mathcal{G}} \sum_{t \in \mathcal{T}} \left[C_g^{LV} e_{gt} + C_g^{NL} u_{gt} + C_g^{SU'} v_{gt} + C_g^{SD'} w_{gt} \right] \tag{18}$$

where $C^{SU'}$ and $C^{SD'}$ are defined as (see Sect. 3.4):

$$C_g^{SU'} = C_g^{SU} + C_g^{NL} SU_g^D \quad \forall g \tag{18a}$$

$$C_g^{SD'} = C_g^{SD} + C_g^{NL} SD_g^D \quad \forall g. \tag{18b}$$

The proposed formulation also takes into account variable startup costs, which depend on how long the unit has been offline. The reader is referred to [17] for further details.

System-wide constraints

Power demand balance and reserve requirements are guaranteed as follows:

$$\sum_{g \in \mathcal{G}} \widehat{p}_{gt} = \sum_{b \in \mathcal{B}} (D_{bt} - p_{bt}^W) \quad \forall t \tag{19}$$

$$\sum_{g \in \mathcal{G}} r_{gt}^+ \geq D_t^+ \quad \forall t \tag{20}$$

$$\sum_{g \in \mathcal{G}} r_{gt}^- \geq D_t^- \quad \forall t, \tag{21}$$

where (19) is a power balance at the end of hour t . The energy balance for the whole hour is automatically achieved by satisfying the power demand at the beginning and end of each hour, and by considering a piecewise linear power profile for demand and generation [14, 18].

Power-flow transmission limits are ensured with [21]:

$$-\bar{F}_l \leq \sum_{g \in \mathcal{G}} \Gamma_{lg}^G \hat{p}_{gt} + \sum_{b \in \mathcal{B}} \Gamma_{lb} \left(p_{bt}^W - D_{bt} \right) \leq \bar{F}_l \quad \forall l, t. \tag{22}$$

Individual unit constraints

The commitment, startup/shutdown logic and the minimum up/down times are guaranteed with:

$$u_{gt} - u_{g,t-1} = v_{gt} - w_{gt} \quad \forall g, t \tag{23}$$

$$\sum_{i=t-TU_g+1}^t v_{gi} \leq u_{gt} \quad \forall g, t \in [TU_g, T] \tag{24}$$

$$\sum_{i=t-TD_g+1}^t w_{gi} \leq 1 - u_{gt} \quad \forall g, t \in [TD_g, T]. \tag{25}$$

The power production and reserves must be within the power capacity limits:

$$\begin{aligned} p_{gt} + r_{gt}^+ &\leq (\bar{P}_g - \underline{P}_g) u_{gt} - (\bar{P}_g - SD_g) w_{g,t+1} + (SU_g - \underline{P}_g) v_{g,t+1} \quad \forall g, t \\ p_{gt} - r_{gt}^- &\geq 0 \quad \forall g, t. \end{aligned} \tag{26}$$

Ramping capability limits are ensured with:

$$\left(p_{gt} + r_{gt}^+ \right) - p_{g,t-1} \leq RU_g \quad \forall g, t \tag{27}$$

$$-\left(p_{gt} - r_{gt}^- \right) + p_{g,t-1} \leq RD_g \quad \forall g, t. \tag{28}$$

By modeling the generation output p_{gt} above \underline{P}_g , the proposed formulation avoids introducing binary variables into the ramping constraints (27) and (28). In other words, when the generation output variable is defined between 0 and \underline{P}_g , then the ramping constraints should consider the case when a generator’s output level should not be limited by the ramp rate, when it is starting up or shutting down; such complicating situations are usually tackled by introducing big-M parameters together with binary variables into the ramping constraints, e.g., [1, 4].

The total power and energy production for thermal units are obtained as follows:

$$\widehat{p}_{gt} = \underline{P}_g (u_{gt} + v_{g,t+1}) + p_{gt} \quad \forall g \in \mathcal{G}^Q, t \quad (29)$$

$$\begin{aligned} \widehat{p}_{gt} = & \underline{P}_g (u_{gt} + v_{g,t+1}) + p_{gt} + \sum_{i=1}^{SU_g^D} P_{gi}^{SU} v_{g,t-i} + SU_g^D + 2 \\ & + \sum_{i=2}^{SD_g^D+1} P_{gi}^{SD} w_{g,t-i+2} \quad \forall g \in \mathcal{G}^S, t \end{aligned} \quad (30)$$

$$e_{gt} = \frac{\widehat{p}_{g,t-1} + \widehat{p}_{gt}}{2} \quad \forall g, t. \quad (31)$$

Wind production limits are represented by:

$$p_{bt}^W \leq P_{bt}^W \quad \forall b, t. \quad (32)$$

Finally, non-negative constraints for all decision variables are:

$$p_{gt}, r_{gt}^+, r_{gt}^- \geq 0 \quad \forall g, t \quad (33)$$

$$p_{bt}^W \geq 0 \quad \forall b, t. \quad (34)$$

References

1. Carrion M, Arroyo J (2006) A computationally efficient mixed-integer linear formulation for the thermal unit commitment problem. *IEEE Trans Power Syst* 21(3):1371–1378. doi:10.1109/TPWRS.2006.876672
2. Damci-Kurt P, Kucukyavuz S, Rajan D, Atamturk A (2013) A polyhedral study of ramping in unit commitment. Research report BCOL.13.02 IEOR, University of California-Berkeley. <http://ieor.berkeley.edu/~atamturk/pubs/ramping.pdf>
3. ERCOT (2011) White Paper functional description of core market management system (MMS) applications for look-ahead SCED, version 0.1.2. Tech. rep., Electric Reliability Council of Texas (ERCOT), Texas-USA. http://www.ercot.com/content/meetings/mef/keydocs/2012/0228/04_white_paper_funct_desc_core_mms_applications_for_la_sced.doc
4. FERC (2012) RTO Unit Commitment Test System Tech. rep., Federal Energy and Regulatory Commission, Washington DC, USA
5. Frangioni A, Gentile C (2006) Solving nonlinear single-unit commitment problems with ramping constraints. *Operat Res* 54(4):767–775. doi:10.1287/opre.1060.0309
6. Frangioni A, Gentile C, Lacalandra F (2008) Solving unit commitment problems with general ramp constraints. *Int J Electric Power Energy Syst* 30(5):316–326. doi:10.1016/j.ijepes.2007.10.003
7. Frangioni A, Gentile C, Lacalandra F (2009) Tighter approximated MILP formulations for unit commitment problems. *IEEE Trans Power Syst* 24(1):105–113. doi:10.1109/TPWRS.2008.2004744
8. Garcia-Gonzalez J, San Roque A, Campos F, Villar J (2007) Connecting the intraday energy and reserve markets by an optimal redispatch. *IEEE Trans Power Syst* 22(4):2220–2231. doi:10.1109/TPWRS.2007.907584
9. Gentile C, Morales-Espana G, Ramos A (2014) A tight MIP formulation of the unit commitment problem with start-up and shut-down constraints. Technical report IIT-14-040A, Institute for Research in Technology (IIT). www.optimization-online.org/DB_FILE/2014/07/4433.pdf
10. Guan X, Gao F, Svoboda A (2000) Energy delivery capacity and generation scheduling in the deregulated electric power market. *IEEE Trans Power Syst* 15(4):1275–1280. doi:10.1109/59.898101

11. Hobbs BF, Rothkopf MH, O'Neill RP, Chao HP (2001) The next generation of electric power unit commitment models, 1st edn. Springer, Berlin
12. Lee J, Leung J, Margot F (2004) Min-up/min-down polytopes. *Discret Optim* 1(1):77–85. doi:[10.1016/j.disopt.2003.12.001](https://doi.org/10.1016/j.disopt.2003.12.001)
13. Meibom P, Barth R, Hasche B, Brand H, Weber C, O'Malley M (2011) Stochastic optimization model to study the operational impacts of high wind penetrations in Ireland. *IEEE Trans Power Syst* 26(3):1367–1379. doi:[10.1109/TPWRS.2010.2070848](https://doi.org/10.1109/TPWRS.2010.2070848)
14. Morales-España G (2014) Unit commitment: computational performance, system representation and wind uncertainty management. Ph.D. thesis, Pontifical Comillas University, KTH Royal Institute of Technology, and Delft University of Technology, Spain
15. Morales-España G, Garcia-Gonzalez J, Ramos A (2012) Impact on reserves and energy delivery of current UC-based Market-Clearing formulations. In: European energy market (EEM), 2012 9th international conference on the, pp. 1–7. Florence, Italy. doi:[10.1109/EEM.2012.6254749](https://doi.org/10.1109/EEM.2012.6254749)
16. Morales-España G, Latorre JM, Ramos A (2013) Tight and compact MILP formulation for the thermal unit commitment problem. *IEEE Trans Power Syst* 28(4):4897–4908. doi:[10.1109/TPWRS.2013.2251373](https://doi.org/10.1109/TPWRS.2013.2251373)
17. Morales-España G, Latorre JM, Ramos A (2013) Tight and compact MILP formulation of start-up and shut-down ramping in unit commitment. *IEEE Trans Power Syst* 28(2):1288–1296. doi:[10.1109/TPWRS.2012.2222938](https://doi.org/10.1109/TPWRS.2012.2222938)
18. Morales-España G, Ramos A, Garcia-Gonzalez J (2014) An MIP formulation for joint market-clearing of energy and reserves based on ramp scheduling. *IEEE Trans Power Syst* 29(1):476–488. doi:[10.1109/TPWRS.2013.2259601](https://doi.org/10.1109/TPWRS.2013.2259601)
19. Padhy N (2004) Unit commitment—a bibliographical survey. *IEEE Trans Power Syst* 19(2):1196–1205. doi:[10.1109/TPWRS.2003.821611](https://doi.org/10.1109/TPWRS.2003.821611)
20. Rajan D, Takriti S (2005) Minimum up/down polytopes of the unit commitment problem with start-up costs. Research report RC23628, IBM. <http://domino.research.ibm.com/library/cyberdig.nsf/1e4115aea78b6e7c85256b360066f0d4/cdcb02a7c809d89e8525702300502ac0?OpenDocument>
21. Shahidehpour M, Yamin H, Li Z (2002) Market operations in electric power systems: forecasting, scheduling, and risk management, 1st edn. Wiley-IEEE Press, New York
22. Stoft S (2002) Power system economics: designing markets for electricity, 1st edn. Wiley-IEEE Press, New York
23. Tahanan M, Ackooij WV, Frangioni A, Lacalandra F (2015) Large-scale unit commitment under uncertainty. *4OR* pp. 1–57 (2015). doi:[10.1007/s10288-014-0279-y](https://doi.org/10.1007/s10288-014-0279-y)
24. Williams HP (2013) Model Building in mathematical programming, 5th edition edn. Wiley, New York
25. Wolsey, L.: Integer Programming. Wiley-Interscience (1998)
26. Yamin HY (2004) Review on methods of generation scheduling in electric power systems. *Electric Power Syst Res* 69(2–3):227–248. doi:[10.1016/j.epsr.2003.10.002](https://doi.org/10.1016/j.epsr.2003.10.002)